NUMERICAL SIMULATION OF THERMAL STORAGE BY LATENT AND SENSIBLE HEAT IN A POROUS VERTICAL CHANNEL: PERFORMANCE ANALYSIS AND COMPARISON

W. FOUDHIL[1], B. DHIFAOUI[2], S. BEN JABRALLAH[3],
Y. DUTIL[4,§]; D. R. ROUSSE[4]

[1] Faculté des Sciences de Tunis, LETTM, Tunis, Tunisia
[2]Institut Supérieur des Sciences et de Technologie de l'Energie, Gafsa, Tunisia
[3]Faculté des Sciences de Bizerte. Bizerte, Tunisia
[4] Chaire de recherche industrielle en technologie de l'énergie et en efficacité énergétique, École de Technologie Supérieure, Montréal, Canada
[§]Correspondence author. Tel: +1 514 396-8462. Email*: yvan@t3e.info*

Abstract

This work proposes a two-dimensional numerical analysis of storage material properties– thermal mass and energy density – in a vertical channel filled with porous media for two storage modes : sensible and latent. The porous channel, into which air flows at low speed, is limited by two walls: one is heated with a constant uniform heat flux while the other is assumed to be adiabatic. The conservation equations, using a model with two temperatures and involving the Darcy-Brinkman law, describe the behavior of the simplified system. The mathematical model thus formed is solved using COMSOL. Glass beads (sensible) and especially encapsulated PCMs (latent) where investigated. Numerical simulations showed that latent heat provides the advantage of improving the thermal inertia and the energy density of the system while controlling the temperature of the porous domain.

Keywords: Porous media, energy storage, sensible heat, latent heat, numerical analysis, PCM.

NOMENCLATURE

A	geometrical shape factor [-]
a_{fp}	contact area solid-fluid [m^2]
c_p	Specific heat at constant pressure [$J.kg^{-1}.K^{-1}$]

Cp_{eq}	Effective volumetric heat capacity [$J.m^{-3}.K^{-1}$]
d	bead diameter [m]
D	temperature transition [K^{-1}]
g	gravitational acceleration [$N.kg^{-1}$]
H	channel height [m]
F	local melt fraction of PCM [-]
h	heat exchange coefficient [$W.m^{-2}K^{-1}$]
h_{fp}	convective heat transfer coefficient solid-fluid [$W.m^{-2}K^{-1}$]
K	permeability [m^2]
L	channel width [m]
L_{fus}	PCM latent heat of fusion [$J.kg^{-1}$]
m_f	mass flow of the fluid at the channel entrance [$kg.s^{-1}$] ($m_f = \rho_f V_0 S$)
P	pressure [Pa]
Pr	Prandlt number[-]
$\dot{q}_w$	heat flux density at the wall [$W.m^{-2}$]
S	entrance area [m^2]
t	time [s]
T	temperature [K or °C]
T_{fus}	melting point of PCM [K or °C]
u, v	velocity components [$m.s^{-1}$]
V	volume[m^3]
(x, y)	cartesian coordinates [m]
X_{VF}	melt volume fraction (average) [-]
SHS	sensible heat storage
$LSHS$	latent and sensible heat storage

Subscripts

a	ambient
d	domain
e	entrance

f	fluid (air)
p	beads
s	solid PCM
l	liquid PCM
w	wall
eq	effective (PCM)
eff	effective (Porous media)
m	average

Greek symbols

ε	porosity [-]
β	thermal expansion coefficient [K^{-1}]
λ	thermal conductivity [$W.m^{-1}.K^{-1}$]
μ	dynamic viscosity [Pa.s]
ν	kinematic viscosity [$m^2.s^{-1}$]
ρ	density [$kg.m^{-3}$]
η	efficiency [-]
χ	storage energy density [$kg.m^{-3}$]

1. INTRODUCTION

The world energy situation has prompted scientists to explore new ways of using the solar energy which has a double advantage of being free and clean but the disadvantage of being intermittent and unsteady. Moreover, in most cases the “offer” and “demand” in thermal energy do not coincide in time. Hence, the obvious key to solve both problems is an efficient storage for low temperature thermal energy.

A channel having a wall exposed to solar radiation can capture energy that can in turn be transmitted to a fluid. This is the common working principle of various thermal solar collector systems, both air- or water-based. To enhance the heat exchanges, the channel could in turn be filled with a porous medium [1, 2]. For fluid and porous media, energy collected can be stored in specially designed reservoirs[3,4,5] as latent heat, or as sensible heat or even both at once[6, 7].

Natural convection in a vertical porous channel heated by the wall has been studied experimentally in our previous work [8]. In that study, investigators have analyzed energy storage by sensible heat, and it showed that the studied system had a high thermal inertia which results in a long period of destocking. The effectiveness of the system, defined as the ratio of energy stored on the energy provided, increased with the storage volume and decreased with the discharge time.

1.1. Phase Change Materials (PCM)

Phase change materials (PCM) can conveniently be used in solar applications since such materials have high storage capacities in small volumes and because they, theoretically, deliver energy at a constant known temperature [9, 10]. Several authors have focused on the use of phase change materials for energy storage [9, 11, 12, 13].

Experimental and numerical studies were conducted by a team involving one of the authors of the current study [12, 14, 15, 16]. The whole work involves a database for multiple phase change materials and examines their behavior to characterize them. These works also model the phenomena of heat transfer and storage / removal of heat with phase change.

Paraffin is often used as a phase change material, given its ease of handling, non-toxicity, life cycle, and adaption to temperatures commonly observed in building applications. Several properties of the latent heat storage for low temperatures are described in various studies [13, 17, 18].

In most cases, except for a few applications of water-ice transformation, the PCM must be encapsulated [11]. The two main reasons are to prevent the leakage of the liquid phase of PCM (to prevent environment contamination) and to have the option of using a heat transfer fluid through a packed bed. Packed beds are advantageous to retrieve or deposit heat since most PCMs involve a very low conductivity. In most situations, the surface area to volume ratio must be increased as much as possible.

1.2. Encapsulated PCM

Most models for latent heat storage in porous media (packed bed) have been produced in the context where the source of heat or cold is external to the porous medium and carried by a fluid. This is somewhat different from the model described here, because in the current case, the heat is applied directly to one of the wall of the porous medium. Hence, its behavior cannot be directly compared to others analyses of heat transfer in porous media. Nevertheless,

these studies may, by analogy, shed some light on this work.

An early study on heat transfer in porous media with PCM has been produced by Saitoh and Hirose [19]. This study showed that, while the porous medium allows better heat transfer between the fluid and the PCM, this comes at the cost of significant pressure drop and increased construction complexity.

Chen et al. [20, 21] have developed a one-dimensional model for a porous medium. The predictions obtained with this model were compared to those embedding a model of lumped capacitances where the temperature is uniform within the capsules and in the coolant, and also with experimental data from literature. This comparison showed that the suggested one-dimensional model allowed the calculation of the temperature distribution in the capsules and in the fluid.

Ismail and Stuginsky [22] compared four groups of models: continuous solid phase model, Schuman's model [23], the single phase model, and a model of thermal diffusion. They found that these models were essentially equivalent except for the computational time.

Zhang et al. [24] developed a general model describing the melting and crystallization of phase change materials in porous media. This model is based on the effective filling factor which is known from the geometry and on the nature of fluid flow, which greatly simplifies the computational complexity.

Arkar and Medved [25, 26] carried experimental and numerical studies of the latent heat storage in a cylinder filled with capsules containing paraffin. These studies examined the influence of the accuracy of the thermal properties of the PCM on the numerical results, identify the parameters that influence the system thermal response and determine the optimum phase change temperature.

An experimental and numerical study by Regin et al. [27] dealing with heat storage in cylindrical capsule containing a PCM showed that the process of melting is mainly controlled by changes of Stefan's number, the range of the melting temperatures and size of the capsules. Thus, it takes less time for the small capsules and for low Stefan's numbers to melt completely and under those circumstances the heat flux is larger.

Benmansour et al. [5] studied the behavior of a reservoir made of randomly located spheres filled with paraffin. The numerical model was validated using experimental results. These tests showed that the loading time of the storage system decreases with the mass flow rate of air. Subsequently, a numerical study proposed by Benmansour [28] showed that the use of three phase change materials instead of one results in a significant energy gain.

A similar study had been produced previously by Watanabe et al. [29, 30] who studied

the impact of the use of phase change materials with different melting points. Numerical and experimental data showed that the mixture of phase change materials improves the exergetic efficiency and reduces the charge and discharge times of the system.

In a series of studies, Bédécarrats et al. [31, 32, 33] and Kousksou et al. [34, 35] analyzed the behavior of a heat storage unit using encapsulated phase change material. The best results were obtained with a vertically oriented system where the natural and forced convection were in the same direction. Also, the charging and discharging rates increase with the flow of heat transport fluid.

Regin et al. [36] propose a numerical study to examine the effect of several parameters on the phenomena of charging and discharging of a cylindrical porous bed consisting of capsules filled with PCM through which water flows. Among their findings, they showed that the duration of complete solidification is greater than the melting time and this is due to low coefficient of heat transfer during solidification. This asymmetric behavior of the phase transition has been observed by several authors in many system configurations [9].

Before closing this section, it should be mentioned that the heat storage system studied here involves many similarities with a Trombe wall using a PCM as an absorber. Various studies of these systems have been carried out in the past (see Zalewski et al. [14] and references therein). As a rule of thumb such a system presents a higher energy density, a shorter discharge time, and a higher efficiency than its equivalent in concrete. While, the geometry of these systems is different from that involved here, the function of both systems is similar. This difference will illustrate the impact of geometry on the thermal behavior of the system.

1.3. Objective of this work

In this work, the behavior of a channel filled with a porous medium and through which air flows from the bottom of the channel under a mixed convection is considered. One of the vertical walls of the channel is subjected to heating at constant and uniform rate while the opposite wall is kept adiabatic.

The main objective of this work is to explore two ways of storing energy in the system described above, and then compare them. The first way is to accumulate heat in sensible form in a porous volume filled with glass beads. The second way is to store heat in capsules containing a phase change material by melting them and then to return this energy to the environment by subsequent solidification. The influence of several system parameters on the

displacement of the melting front and the temperature profile is examined. From this model the primary goal is to improve the energy stored per unit volume in the channel and the thermal inertia of the reservoir.

To achieve this goal, a mathematical model for the energy stored in the porous volume by sensible and latent heat is formulated. Then, this formulation is implemented (here in a commercial code, COMSOL). Finally, the combined formulation and implementation are validated by use of common tests for consistency, stability, convergence, and grid independence. Once the tool is ready, it is used to first predict results for which experimental values were obtained, then to carry-out parametric studies.

The complexity of the problem lies in two aspects:

- The definition of the appropriate expression for the energy stored in a partially melted medium. This task requires knowledge of the volume fraction of melt.
- The combination of two physical phenomena in the same environment: heat transfer in porous media and thermal behavior of a phase change material encapsulated in the solid matrix.

2. MATHEMATICAL MODEL

In this investigation the three-dimensional solar wall involving storage materials is modeled such that the width (aligned with the *z*-axis) is very large compared to the thickness (aligned with *x*) such that attention is focused on the mid plane of the solar wall. Hence, the three dimensional problem is assumed, for the purpose of this first study, as a two-dimensional domain in *x* and *y* (Fig.1). In Figure 1, the left-hand side is assumed to involve a constant and uniform heat flux, the right-hand side is supposed to be perfectly adiabatic, and the incoming temperature and velocity distributions are assumed to be known at the bottom.

This paper proposes an investigation of the fluid dynamics and heat transfer in this geometry considered to be filled with a porous medium consisting of two phases : a fluid phase (air that flows from the bottom to the top) and a rigid solid phase (spherical beads of either glass or PCM) (Fig.1).

INSERT FIG 1 ABOUT HERE

The governing equations written at the macroscopic scale are averaged equations based on the method suggested by Whitaker [37]:

Continuity equation

$$\frac{\partial u}{\partial x}+\frac{\partial v}{\partial y}=0 \tag{1}$$

Darcy-Brinkman equation along the vertical axis (*Oy*)

$$\frac{\rho_f}{\varepsilon}\frac{\partial v}{\partial t}+\frac{\mu_f}{K}v=-\frac{\partial p}{\partial y}+\rho_f g+\frac{\mu_f}{\varepsilon}\left(\frac{\partial^2 v}{\partial x^2}+\frac{\partial^2 v}{\partial y^2}\right) \tag{2}$$

Darcy-Brinkman equation along the horizontal axis (*Ox*)

$$\frac{\rho_f}{\varepsilon}\frac{\partial u}{\partial t}+\frac{\mu_f}{K}u=-\frac{\partial p}{\partial x}+\frac{\mu_f}{\varepsilon}\left(\frac{\partial^2 u}{\partial x^2}+\frac{\partial^2 u}{\partial y^2}\right) \tag{3}$$

Conservation of energy for the fluid (air)

$$\varepsilon(\rho c_p)_f\frac{\partial T_f}{\partial t}+(\rho c_p)_f\left(u\frac{\partial T_f}{\partial x}+v\frac{\partial T_f}{\partial y}\right)=\varepsilon\lambda_f\left(\frac{\partial^2 T_f}{\partial x^2}+\frac{\partial^2 T_f}{\partial y^2}\right)-h_{fp}a_{fp}(T_f-T_p) \tag{4}$$

Conservation of energy for the beads:

$$(1-\varepsilon)(\rho c_p)_p\frac{\partial T_p}{\partial t}=(1-\varepsilon)\lambda_p\left(\frac{\partial^2 T_p}{\partial x^2}+\frac{\partial^2 T_p}{\partial y^2}\right)+h_{fp}a_{fp}(T_f-T_p) \tag{5}$$

When capsules containing a phase change material are used as beads, the thermophysical properties are different for the solid and liquid phases. To mathematically describe this behavior, a variable *F* that is related the phase of the MCP, is employed. *F* is conveniently set to 0 for the solid phase and to 1 for the liquid phase.

The transition of *F* from 0 to 1 requires the use of a function within the formulation (here a smoothed Heaviside function has been chosen [9]) to avoid numerical instability.

Then, equation (5) is slightly modified and takes the form:

$$(1-\varepsilon)Cp_{eq}\frac{\partial T_p}{\partial t}=(1-\varepsilon)\lambda_{eq}\left(\frac{\partial^2 T_s}{\partial x^2}+\frac{\partial^2 T_p}{\partial y^2}\right)+h_{fp}a_{fp}(T_f-T_p) \tag{6}$$

Here, it is important to specify that Cp_{eq} and λ_{eq} represent the "effective" or equivalent volumetric heat capacity and thermal conductivity of the combined solid and liquid PCM, respectively. These values are simply assumed to be linear interpolations of the values of the same parameter for the solid and liquid phases such that:

$$Cp_{eq}=F\rho_l(c_p)_l+(1-F)\rho_s(c_p)_s+DL_{fus}(F\rho_l+(1-F)\rho_s) \tag{7}$$

$$\lambda_{eq}=F\lambda_l+(1-F)\lambda_s \tag{8}$$

In eq. (7), $c_{p,l}$ and $c_{p,s}$ represent the specific heat capacity while in eq.(8), λ_l and λ_s

represent the thermal conductivity of the liquid and the solid phases, respectively. Therefore:

When F=0 (solid PCM): $Cp_{eq} = \rho_s (c_p)_s + DL_{fus}\rho_s$ and $\lambda_{eq} = \lambda_s$

When F=1 (liquid PCM): $Cp_{eq} = \rho_l (c_p)_l + DL_{fus}\rho_l$ and $\lambda_{eq} = \lambda_l$

Here, D is a temperature transition [K^{-1}]. The pulse D is the derivative of F with respect to temperature.

The latent heat of fusion $L_{fus}$is defined as a pulse about the temperature transition D. The integral of D is by definition equal to unity, such that:

$$\int_{-\infty}^{\infty} \rho DL_{fus} dT = \rho L_{fus} \tag{9}$$

The characteristic variables defined by equations (1–6) [38,39,40,41] are the permeability of the porous medium, K, the convective heat transfer coefficient for fluid-particles interaction, h_{fp}, and the fluid-particles contact area, a_{fp}. These three variables can be expressed as:

$$K = \frac{d^2 \varepsilon^3}{150(1-\varepsilon)^2} \tag{10}$$

$$h_{fp} = \frac{\lambda_f}{d}\left[2 + 1.1 Pr_f^{0.33}\left(\frac{vd}{\nu_f}\right)^{0.6}\right] \tag{11}$$

$$a_{fp} = \frac{6(1-\varepsilon)}{d} \tag{12}$$

The initial conditions are for velocity and temperature are given by the standard expressions:

$$t = 0: \quad u = v = 0, \quad T_f = T_p = T_a, \tag{13}$$

where T_a is the ambient temperature.

The thermal and velocity boundary conditions in the porous medium are given by [42,43]:

$$y = 0: u = 0,\ v = V_e,\ T_f = T_e,\ (1-\varepsilon)\lambda_p \frac{\partial T_p}{\partial y} = h_{fp}(T_p - T_e), \tag{14}$$

$$y = H: \quad \frac{du}{dy} = \frac{dv}{dy} = 0, \quad \frac{\partial T_f}{\partial y} = \frac{\partial T_p}{\partial y} = 0, \tag{15}$$

$$x = L: \quad u = v = 0, \quad \frac{\partial T_f}{\partial x} = \frac{\partial T_p}{\partial x} = 0, \tag{16}$$

$$x = 0 : u = v = 0,\ \dot{q}_w = -\lambda_f \left(\frac{\partial T_f}{\partial x}\right)_w = -\lambda_p \left(\frac{\partial T_p}{\partial x}\right)_w, \quad (17)$$

Here, T_e and V_e are the temperature and velocity at the entrance of the porous domain, respectively.

In eq. (17), the value of the heat flux on the left-hand side wall varies throughout the cycles: first, $\dot{q}_w \neq 0$ while the material is heated and therefore melts. Then, no flux is applied, that is $\dot{q}_w = 0$, in the discharge phase, when the PCM solidifies.

The transient regime was considered as evidenced by the time derivatives involved in the above-mentioned mathematical description of the problem. The description of the transfer in porous media is obtained by solving the system formed by equations (1-5). When the spheres are replaced by the capsules containing the PCM, equation (5) is simply replaced by equation (6).

3. STORED ENERGY FORMULATION

3.1. Sensible heat storage

To express the heat stored in the porous medium, we adopt the hypothesis of local thermal equilibrium. Thus, for a change in average temperature *dT*, the stored energy can be expressed by:

$$dE_{sen} = mc_{p,eff}\, dT = \left(\rho c_p\right)_{eff} V dT \quad (18)$$

The energy stored in the whole medium E_{sen} is given by the integral:

$$E_{sen} = \int_{T_a}^{T_{md}} V \left(\rho c_p\right)_{eff} dT \quad (19)$$

T_a and T_{md} are the initial and final average temperature of the porous medium.

V represents the total volume of the porous medium.

$(\rho c_p)_{eff}$ is the volumetric effective heat content of the porous domain given by :

$$(\rho c_p)_{eff} = (1-\varepsilon)(\rho c_p)_p + \varepsilon(\rho c_p)_f \quad (20)$$

3.2. Latent and sensible heat storage

Through the phase change, the calculation of the stored energy must take into account the sensible heat and latent heat. Indeed, under the effect of heating, a fraction of the porous

medium undergoes a phase change while the rest temperature increases without reaching the melting point. The stored energy takes different forms. To express this, we use the variable X_{VF} characterizing the volume fraction of molten porous medium, defined by:

$$X_{VF} = \frac{V_{PCM(fus)}}{V_{PCM}} \tag{21}$$

$V_{PCM(fus)}$ and V_{PCM} represent the melted volume and the total volume of PCM in capsule, respectively. Knowing that $V_{PCM} = (1-\varepsilon)V$ (the capsule wall thickness is neglected), then V and ε represent the total volume of the porous medium and its porosity.

3.2.1. Energy stored with PCM capsules

To express the energy storage in capsules, three stages X_{VF} are considered:

1. This stage occurs when the temperature of a solid PCM rises from its initial temperature until a portion of it, $X_{VF}V_{PCM}$, reaches the melting point. Meanwhile, the other part of the PCM, $(1-X_{VF})V_{PCM}$, does not reach the required temperature for phase change. So there is simultaneously sensible and latent heat storage.
2. This phase corresponds to the storage dominated by the phase change of the PCM in the molten part $X_{VF}V_{PCM}$, which must be added to the contribution of sensible heat stored in the unmelted solid phase $(1-X_{VF})V_{PCM}$.
3. At the end of this phase, the complete volume $X_{VF}V_{PCM}$ has melted; its temperature is above the melting temperature $(T_{m1} > T_{fus})$, while the other part $(1-X_{VF})V_{PCM}$ remains solid and has a temperature $T_{m2} < T_{fus}$. This phase corresponds to the period of storage by sensible heat.

As a consequence, to account for these possibilities, the energy stored in PCM capsule is expressed such that:

Within the melt volume fraction X_{VF}:

$$E_1 = \int_{T_a}^{T_{fus}} (\rho c_p)_s (X_{VF}V_{PCM})dT + \rho_l (X_{VF}V_{PCM})L_{fus} + \int_{T_{fus}}^{T_{m1}} (\rho c_p)_l (X_{VF}V_{PCM})dT \tag{22}$$

with $T_{m1} > T_{fus}$.

In the solid fraction $(1-X_{VF})$:

$$E_2 = \int_{T_a}^{T_{m2}} (\rho c_p)_s \left[(1 - X_{VF}) V_{PCM} \right] dT \tag{23}$$

with $T_{m2} < T_{fus}$.

Total energy stored in the PCM is simply the total of both:

$$E_{PCM} = E_1 + E_2 \tag{24}$$

In the previous equations, ρ_s, ρ_l, $c_{p,s}$ and $c_{p,l}$ are, respectively, the densities and specific heats for both solid and liquid phases, T_{m1} is the average final temperature of the melted fraction, X_{VF}, T_{m2} represent the average final temperature of the unmelted fraction, $1 - X_{VF}$, T_a is the ambient temperature, and T_{fus} is the melting point of PCM.

3.2.2. Energy stored in air

The sensible heat stored in the air passing through the porous medium E_f is equal to:

$$E_f = \int_{T_a}^{T_{mf}} (\rho c_p)_f V_f dT \tag{25}$$

T_{mf} is the average temperature of the air in the stationary regime.

V_f is the volume occupied by the air in the porous domain $V_f = \varepsilon V$

3.2.3.Total energy stored

By adding the energy stored within the porous medium and the air, the total energy stored in the domain formed by the porous spherical particles filled with a PCM and crossed by air is obtained:

$$E_{lat} = E_{PCM} + E_f \tag{26}$$

3.3. Energy density

The storage energy density χ [J·m^{-3}] is the amount of heat stored by unit of volume and defined by:

$$\chi = \frac{E}{V} \tag{27}$$

with E and V the energy stored in the porous medium and the total volume of the porous medium.

4.NUMERICAL SOLUTION

4.1.A commercial code

Numerical solutions of the system of equations are obtained using COMSOL Multiphysics. This code uses a discretization and a formulation based on the finite element method.

4.2. Numerical details

The numerical core of COMSOL consists of a family of solvers to balance equations. In this study, unsteady fluid flow and heat transfer is solved. Therefore, the software proposes by default to solve simultaneously the unknowns (U, P, T_f and T_P) in the discretized system of equations. To account for the physics of phase change, the software provides an equation that permits to introduce the liquid and solid properties of the PCM and the equivalent thermal properties. Here, convergence is ensured by successive iterations through each time step. In the proposed analyses, it was found that the convergence is satisfied by use of the default values for the absolute (0.001) and the relative tolerances (0.01). No further gain was obtained with tighter constraints.

The mesh considered is a non-uniform grid made of various size triangular elements with refinement in the areas involving the sharpest gradients and/or close to the boundaries.

4.3. Validation

After several preliminary tests for consistency, stability, convergence, and grid independence, the optimal grid and geometry were validated by comparison with experimental results obtained by Dhifaoui et al. [8] in the case of a channel filled by a porous medium. Fig. 2 shows the variation of the temperature with time in the immediate vicinity of the heated (left) boundary. In Fig. 2, the numerical predictions are a bit above the experimental curve because the perfect insulation is only possible numerically. Nevertheless, the maximum difference in temperature with time is only 3.5 ^{o}C. This provides confidence in the model.

INSERT FIG 2 ABOUT HERE

5. RESULTS AND DISCUSION

The operational conditions are described by the following parameters: the temperature

and the flow at the channel entrance, and the diameter of the beads d .

5.1. Sensible Heat Storage

In this section, the accumulation of energy in a porous vertical channel filled with solid spherical glass beads into which air flows is investigated. In the absence of fusion, energy is only stored as sensible heat. The characteristics of the porous medium are summarized in Table1.

INSERT TABLE 1 ABOUT HERE

The model provides the temperature for each component (fluid and particle) of the porous medium. The evolution of the average temperature for the case of glass beads during the charge and discharge processes is illustrated in Fig.3.In this test case the heat flux on the left-hand-side is $\dot{q}_w = 250\ \mathrm{Wm}^{-2}$ for the first half of the process (57,600 s or 16 hours) while it is set to zero afterwards. The cavity aspect ratio is $A = 5$, the bead diameter is $d = 10^{-2} m$, the mass flow rate is $m_f = 1.2 \times 10^{-4}\ \mathrm{kg \cdot s^{-1}}$, $T_e = 298\ \mathrm{K}$.

In this section, the effect of this variation on the thermal inertia of the system and the energy density χ is examined. Note that the channel height is *H*, width is L, and aspect ratio is $A=H/L$. Figure 3 and 4 show the variations in average temperature of the particle domain, T_p., with respect to time for variations in height, width, and domain volume. The variation of the height of the channel or spacing between the walls leads to a variation in the amount of material in the porous area.

In all cases, it is found that the system has a significant thermal inertia during the charging phase (in terms of hours). To return to the initial state (complete discharge), the system requires almost the same amount of time (to release the heat stored during the charging phase). This particular behavior is confirmed by the experimental work of Dhifaoui et al. [8], who obtained similar results to those presented here. However, in this experimental setup a slight asymmetry was observed between the charge and discharge process. Heat losses and three dimensional effects could explain such discrepancies.

In Figure 3a, the evolution of the average temperature of the system for both charge and discharge, when the height varies and the width is fixed, is presented. This figure indicates that increasing the amount of material in the porous domain by an increase in the height of the channel considerably improves the thermal inertia of the system. This increase in height correspondingly increases the length exposed to the heat flux, bringing more energy into de

system. This in turn increases the maximum temperature and the energy density χ. This also increases the overall mass involved and consequently the thermal inertia.

Note that χ is calculated when the system reaches a steady state.

Fig.3b shows the change in average temperature of the system for both charge and discharge, when the width varies and for a constant height. This curve illustrates that the thermal inertia of the system does not show considerable variation when varying the amount of material in the porous medium by varying its width.

Increasing the width of the domain has two opposing effects: 1) to increase the entrance flow which slows the charging time; 2) to increase the amount of material, without varying the heating surface, which increases the charging time. These two opposite effects lead to invariance of storage time when the width of the domain varies.

Nevertheless, since the heat flux is directed to the adiabatic wall, the average temperature of the system increases when the spacing decreases. And, of course, this causes an increase in energy density χ.

INSERT FIG 3ABOUT HERE

Fig.4 involves the evolution of the average temperature of the system, for the charge process when varying the width L and height H while keeping a constant aspect ratio. It can be observed that increasing the amount of material in the porous area significantly improves the thermal inertia of the system without considerable variation in the average temperature. This may be explained by the fact that the porous medium needs more time to reach the steady state when the height is increased. Nevertheless, the energy density χ remains almost constant for a constant aspect ratio. Indeed, the temperature field does not vary greatly since increases of H and L have antagonistic effects on the thermal state of the system.

INSERT FIG 4ABOUT HERE

When H doubles, so does the heat rate on the left-hand side. But as L also doubles, this in turn allows for doubling the heat convected through the upper boundary leading to similar equilibrium temperature as long as A remains constant.

On the other hand, as both H and L increase simultaneously, with constant d. That, is there is more and more solid compare to air and therefore the equilibrium takes more time to be established as the air capacity is much less than that of the solid particles.

The latter case presents the advantage of improving the thermal inertia without increasing the system temperature, but instead increasing the amount of material in the channel. The property is useful in building application where the temperature in the system

should not exceed a certain level for reasons of comfort.

The porous vertical channel filled with glass beads into which air is flowing acts as a heat storage system. The thermal behavior of this system can be tailored by acting on its geometry. Nevertheless, the main drawback of such systems remains its bulk. To improve the energy density, we have to increase the amount of material to avoid reaching high temperatures which are not suitable for building applications (above 300-305 K maximum).

5.2. Latent Heat Storage

In this section, the thermal storage by latent and sensible heat is investigated. The system is now composed of capsules containing a phase change material (Fig. 1) that are considered as a porous medium. Four physical phenomena are involved: the transfer of heat by convection, heat transfer by conduction, the energy storage by latent and sensible heat, and the fluid flow through the solid matrix.

The heat transfer inside the capsules (in PCM) is considered to occur only by conduction. Indeed, the volume of PCM in each capsule is rather small so the effects of convection in the molten PCM are considered negligible [27,44,45].

For this analysis, the PCM used is paraffin. Table2 presents the physical characteristics of the selected paraffin.

INSERT TAB 2 ABOUT HERE

5.2.1. Temperature distribution in the porous medium

In Fig. 5, the temperature distribution in the channel over of time during the charging phase is shown for 10 000, 20 000, 30 000 and 40 000 s. The heating of the medium is mainly localized near the heated wall and to the top the canal, where the temperature exceeds the melting temperature of the PCM.

INSERT FIG 5ABOUT HERE

5.2.2. Selected profiles, mass flow rates and inlet temperature

The temperature variation in the phase change material versus time for different sections heights, *y*, is shown in Fig.6a. This curve shows that the PCM does not melt completely and that the phase change occurs mainly in the upper half of the channel. Indeed, the air introduced into the inlet is at room temperature, which is well below the melting temperature of the PCM. So there is a loss of storage efficiency as the fusion does not occur below

$y = 0.15\,\mathrm{m}$. At that height, a temperature plateau, due to the fusion of PCM, is observed.

INSERT FIG 6ABOUT HERE

Fig.6b represents the temporal evolution of the average temperature in the porous medium for various mass flow rates. This figure shows that a reduction of the entrance flow rate (dotted line) increases both the storage period and the storage temperature. Hence, since the fluid needs more time to pass through the porous medium, it has more time to gather heat and transfer it to the storage material.

Fig.6c demonstrates the temporal variation of the average temperature in the porous medium for various entrance temperatures of the fluid. It can be noted that the increase in the entrance temperature improves the thermal inertia, since it favors the fusion of PCMs (see Table 3), which in turn increases the time needed to reach steady state. These results are in agreement with the numerical and experimental works of Bédécarrats et al. [32,33], who concluded that storage duration increases with the entrance temperature and decreases with the fluid flow.

5.2.3 Fusion front and melt volume fraction

The liquid fraction, F, is monitored throughout the channel. The variation of F with time is shown in Fig.7during the charging phase (melting of the PCM). During this phase, the melting front moves toward the cold wall (from left to right) and down the field. Figure 7 confirms that fusion of the PCM does not occur in the lower area of the porous domain (as seen in the previous section).

INSERT FIG 7ABOUT HERE

Fig.8 shows the variation of F at $y=H/2$ depending on the distance from the heated wall and time. During the initial phase of heating, the capsules near the heated wall undergo phase change (melting). Overtime, the melt fraction increases and the melting front moves toward the adiabatic wall.

INSERT FIG 8ABOUT HERE

Fig.9a shows the variation of melted volume fraction, X_{VF}, versus time for different mass flow rates of the fluid. It can be observed that both the melted volume fraction and the energy density increase with decreasing mass flow. Indeed, when reducing the fluid velocity, its temperature raises more as the travel time gets longer.

The change in the melted volume fraction X_{VF} with respect to time for several diameters of the capsules containing phase change material is shown in Fig.9b. It can be observed that an increase in the particle diameter increases X_{VF} and therefore the quantity of

energy stored per unit volume χ .This is the opposite of the behavior reported by Regin et al. [36], who studied the case of a flow of heated water through a porous bed consisting of capsules filled with paraffin. They showed that for a given time during fusion, the melt fraction increases when the diameter of the particles decreases. This apparent contradiction find its explanation in the experimental work of, Jiang et al. [41] and the numerical work Foudhil et al. [46]. Both studies showed that the ratio of particle-fluid conductivity plays an important role on the heat transfer variation with the diameter of the capsules. They indeed showed that when the ratio of conductivities $\lambda_p/\lambda_f \approx 1$ (as in the case studied by Regin et al. [36]) heat transfer – between heated wall and the porous media – increases with the capsule diameter, and that the opposite behavior was observed when $\lambda_p/\lambda_f > 1$, as in the case involved herein. Also, the influence of the diameter of capsule and, hence, on the energy density disappears for large diameters (Fig.10).

INSERT FIG 10 ABOUT HERE

5.3. Performance comparison of both storage systems

The thermal inertia and the energy density in the channel are the parameters characterizing the performance of the investigated energy reservoir. In this section, the performances of heat storage material are compared: sensible heat storage (SHS) in glass beads and latent and sensible heat storage (LSHS) in capsules containing PCM.

5.3.1. Energy density

Tables3, 4 and 5 show the comparison between the values of the energy density for the two storage modes: sensible and sensible-latent, the same time, $t = 5\times10^4$ s. To compare the two storage modes, we adopt an aspect ratio A =5, and require that the wall flux to be equal to $\dot{q}_w = 250\ \mathrm{Wm}^{-2}$. We define ΔT as the temperature difference between the inlet and ambient temperature: $\Delta T = T_e - T_a$

INSERT TAB 3 ABOUT HERE

INSERT TAB 4 ABOUT HERE

INSERT TAB 5 ABOUT HERE

The results of Table3, 4 and the second column of the table 5 demonstrate that the energy density improves when there is combined sensible and latent heat storage. This improvement in energy density is almost constant at about 53% under variation of the inlet

temperature and particle diameter for a fixed mass flow rate ($m_f = 1.2 10^{-4} kg.s^{-1}$). Table 5 indicates that the energy density ratio varies with the mass flow rate. These results bring the conclusion that energy density ratio is essentially controlled by the fluid mass flow rate.

5.3.2. Thermal inertia

Fig.11 presents the comparison of storage and retrieval of heat between a sensible heat storage system (SHS) and a latent heat storage system (LSHS). This curve shows the evolution of the average temperature of the capsules throughout the channel. The results presented in Fig.11 demonstrate that the thermal inertia of the system is improved by use of capsules containing a PCM compared to the storage system using only sensible heat (t_{LSHS} f t_{SHS}).

Moreover, the latent heat storage reduces the average temperature in the system and this presents an advantage for building applications, while this would also reduce the heat loss to the exterior in a Trombe wall, for instance.

INSERT FIG 11 ABOUT HERE

To study the behavior of the system through the charge ($\dot{q}_w = 250\ \mathrm{Wm^{-2}}$) and discharge ($\dot{q}_w = 250\ \mathrm{Wm^{-2}}$), the variation of the average temperature of the system is investigated. Fig. 12a, for glass capsules, and Fig.12b, for PCM capsules, demonstrate that this behavior is not symmetric. These results are similar to those obtained by Dhifaoui et al. [8]. The difference between the curves on each figure can be explained by the presence of hysteresis, which indicate that the behavior is affected by memory of previous perturbations [12,47]. Specifically, the time constant is smaller for the charge than for the discharge cycle.

INSERT FIG 12 ABOUT HERE

Finally, figure 13 describes the evolution of the fluid temperature for three periods of time with respect to the height, *y*, of the cavity in the vertical mid-plane ($x=L/2$). Fig. 13a and 13b correspond to the cavity filled with glass beads and PCM capsules, respectively.

These curves show that the temperature of the medium increases (linearly for the case of glass) with the height of the domain and that for each time t, the presence of MCP reduces the temperature of the fluid within and out of the medium.

6. CONCLUSION

A thorough performance numerical analysis of storage in a porous vertical channel has

been conducted in this study. Two modes of storage were compared: sensible and latent heat storage. As a first step, an analysis of the thermal inertia and energy density through the variation in the amount of sensible heat storage material for different shape factors was carried out. An increase in the height of the channel considerably improves the thermal inertia of the system. This increase in inertia is accompanied by an increase in average temperature and an increase in energy density. However, the thermal inertia of the system is almost insensitive to the spacing between the channel walls. Nevertheless, the average temperature of the system increases when the spacing decreases, causing an increase in energy density χ. Lower mass flow rates increase both average temperature and energy density. Based on those observations, as a general design rule, such storage system should be as tall and slender as possible, while the airflow should be as low as possible. This provides the incentive to study the effects of natural convection in the porous medium.

In the second step, this study showed that storage performance can be improved by use of capsules containing a phase change material without reaching excessive temperatures. Nevertheless, the PCM does not melt completely. Investigators sought to track the movement of the melting front to improve the melt volume fraction, and consequently the energy density of the reservoir. Globally, it has been shown that the melt volume fraction X_{VF} and consequently the energy density χ :

- Increase with the temperature of the fluid channel at the entrance,
- Increase with the particle diameter,
- Decrease with increasing mass flow rate.

The effect of the increase of the diameter of particles on both the melted fraction and energy stored per unit volume diminishes with increasing particle diameter. Overall, the relative improvement of energy density between the two modes is essentially driven by the fluid flow rate.

Compared to the channel filled with solid glass beads, the channel filled with capsules containing a phase change material has the following advantages. It :

- Reduces the temperature,
- Improves the energy density,
- Has a greater thermal inertia.

It is worth noting that, in the lower part of the channel, the PCM is not melting. In consequence, to reduce the overall cost, this lower part might be filled with glass beads with little impact on the storage performance.

This last result contradicts what is generally reported in the literature for PCM use in Trombe walls. Hence, its open the possibility for customizing the performances of Trombe wall involving PCMs by a modification of the geometry and an appropriate distribution of glass and PCM capsules.

REFERENCES

1. M. K. Alkam, M.A. Al-Nimr, and M.O. Hamdan, Enhancing heat transfer in parallel-plate channels by using porous inserts, Int. J. of Heat and Mass Transfer, vol. 44, pp. 931–938, 2001.

2. A. A. Mohamad, Heat transfer enhancements in heat exchangers fitted with porous media. Part I: constant wall temperature, Int. J. of Thermal Sciences, vol. 42, pp. 385–395, 2003.

3. J. Duffie and W. Beckmann, Solar engineering of thermal processes. John Wiley and Sons, New York, 1980.

4. D. E. Beasley and C. Ramanarayan, Thermal response of packed bed of spheres containing a phase change material, Int. J. of Energy Research, vol.13, pp. 253–265, 1989.

5. A. Benmansour and M. A. Hamdan, Simulation du stockage de l´énergie thermique dans un lit fixe de sphères contenant un matériau à changement de phase. Revue Énergie renouvelable, vol. 4, pp.125–134, 2001.

6. J. Millette, Conception, instrumentation, modélisation et analyse d'un élément de stockage d'énergie par chaleur latente. Ph.D. thesis, Université de Sherbrooke, Sherbrooke, Québec, Canada, 1999.

7. M. Amir, Modélisation d'un élément de stockage d'énergie destiné aux planchers chauffants, Ph.D. thesis, Université de Sherbrooke, Sherbrooke, Québec, Canada, 1996.

8. B. Dhifaoui, S. Ben Jabrallah, A. Belghith, and J.P. Corriou, Experimental study of the dynamic behaviour of a porous medium submitted to a wall heat flux in view of thermal energy storage by sensible heat, International journal of thermal sciences, vol.46, pp. 1056–1063, 2007.

9. Y. Dutil, D. R. Rousse, N. Ben Salah and S. Lassue, A Review on Phase Change Materials: Mathematical Modeling and Simulations, RSER, vol.15(1), pp. 112–130, 2011.

10. Y. Dutil, D. R. Rousse, and G. Quesada, Sustainable Buildings: An Ever Evolving Target, Sustainability, vol. 3, pp. 443–464,2011.

11. H. Mehling and L. F. Cabeza, Heat and cold storage with PCM, An up to date introduction into basics and applications, Springer-Verlag, Berlin Heidelberg, Germany, 2008.

12. Z. Younsi, L. Zalewski, D. Rousse, A. Joulin, S. Lassue, A novel technique for the experimental thermophysical characterization of phase change materials, Int. J. Thermophysics, vol. 32, pp. 674–692, 2011.

13. S.M. Husnain, Review on sustainable thermal energy storage technologies, part 1: heat storage materials and techniques. Energy Conv. Manage, vol.39, pp. 1127–1138, 1998.

14. L. Zalewski, A. Joulin, S. Lassue, Y. Dutil and D. Rousse, Experimental study of small-scalled solar wall integrating Phase Change Material, Solar Energy, vol. 86(1), pp. 208–219, 2012.

15. A. Joulin, Z. Younsi, L. Zalewski, S. Lassue, D. Rousse, J.P. Cavrot, Experimental and numerical investigation of a phase change material: Thermal-energy storage and release, Applied Energy, vol. 88(7), pp. 2454–2462, 2005.

16. A. Joulin, Z. Younsi, L. Zalewski, D. Rousse, S. Lassue, A numerical study of the melting of phase change material heated from a vertical wall of a rectangular enclosure Int. J. Comp Fluid Dynamics, vol. 23(7), pp. 553–566, 2009.

17. A. Abhat, Low temperature latent heat thermal energy storage; heat storage materials. Solar energy, vol. 30(4), pp. 313–332, 1983.

18. Z. Belen, MM. Luisa, and M. Harald, Review on thermal energy storage with phase change: materials, heat transfer analysis and applications, App. Therm. Eng. vol. 23, pp. 251–283, 2003.

19. T. Saitoh and K. Hirose, High-performance of phase change thermal energy storage using spherical capsules, Chem. Eng. Commun., vol. 41, pp. 39–58, 1986.

20. S. L., Chen and J. S. Yue, A simplified analysis for cold storage in porous capsules with solidification, ASME J. of Energy. Resour. Technol., vol.113, pp. 108–116, 1991.

21. S. L. Chen, One dimensional analysis of energy storage in packed capsules,ASME J. Sol. Energy. Eng., vol.114, pp.127–130, 1992.

22. K. A. R. Ismail and R. Stuginsky, A parametric study on possible fixed bed models for PCM and sensible heat storage, Appl. Therm. Eng., vol.19, pp. 757–788, 1999.

23. T.E.W. Schumann, Heat transfer: a liquid flowing through a porous prism, J. Franklin Inst., 208, pp. 405-416, 1929.

24. Y. Zhang, S. Yan, Y. Zhu and X. Hu, A General model for analyzing the thermal performance of the heat charging and discharging process of latent heat thermal energy storage systems, Trans ASME J. Sol. Energy Eng., vol. 123, pp. 232–236, 2001.

25. C. Arkar and S. Medved, Influence of accuracy of thermal property data of a phase change material on the result of a numerical model of a packed bed latent heat storage with spheres, Thermochimica Acta, vol. 438, pp.192–201, 2005.

26. C. Arkar and S. Medved, Free cooling of a building using PCM heat storage integrated into the ventilation system, Solar Energy, vol. 81, pp.1078–1087, 2007.

27. A. F. Regin, S.C. Solanki, and J.S. Saini, Latent heat thermal energy storage using cylindrical capsule: Numerical and experimental investigation, Renewable Energy, vol. 31, pp. 2025–2041, 2006.

28. A. Benmansour, Étude numérique du stockage de l´énergie thermique en lit multicouche. 18ème Congrès Français de Mécanique, pp. 27-31, Grenoble, France, 2007.

29. T. Watanabe T, H. Hikuchi and A. Kanzawa, Enhancement of charging and discharging rates in a latent heat storage system by use of PCM with different melting temperature, Heat Recovery Syst. and CHP, vol. 13(1), pp. 57– 66, 1993.

30. T. Watanabe and A. Kanzava, Second law optimization of a latent heat storage system with PCMs having different melting points, Heat Recovery Syst. and CHP, vol. 15(7), pp. 641–653, 1995.

31. J. P. Bédécarrats and J. P. Dumas, Study of the crystallization of nodules containing a phase change material for cool thermal storage, Int J. Heat Mass Transfer, vol. 40(1), pp. 149–157, 1996.

32. J. P. Bédécarrats, J. Castaing-Lasvignottes, F. Strub and J.P. Dumas, Study of a phase change energy storage using spherical capsules. Part I: Experimental results, Energy Conversion and Management, vol. 50, pp. 2527–2536, 2009.

33. J. P. Bédécarrats, J. Castaing-Lasvignottes, F. Strub and J.P. Dumas, Study of a phase change energy storage using spherical capsules. Part II: Numerical modeling, Energy Conversion and Management, vol. 50, pp.2537–2546, 2009

34. T. Kousksou, J. P. Bédécarrats, J. P. Dumas and A. Mimet, Dynamic modeling of the storage of an encapsulated ice tank, Appl. Therm. Eng. vol 25, pp. 1534–1548, 2005.

35. T. Kousksou, J. P. Bédécarrats, F. Strub, J. Castaing-Lasvignottes, Numerical simulation of fluid flow and heat transfer in a phase change thermal energy storage, Int J. Energy Technol. Policy. vol. 6(1/2), pp. 143–158, 2008.

36. A. F. Regin, S.C. Solanki, and J.S. Saini, An analysis of packed bed latent heat thermal energy storage system using pcm capsules: Numerical investigation, Renewable Energy, vol. 34, pp.1765–1773, 2009.

37. S. Whitaker, Simultaneous Heat, Mass and Momentum Transfer in Porous Media, a Theory of Drying, Advances in Heat Transfer, vol.13, pp.119–203, 1977.

38. A. Amiri and K. Vafai, Analysis of dispersion effects and non-thermal equilibrium, non-darcian, variable porosity incompressible flow through porous media, Int. J. of Heat and Mass Transfer, vol. 37, pp. 939–954, 1994.

39. M. Kaviany, Principles of Heat Transfer in Porous Media. Second Edition, Springer-Verlag, New York, 1999.

40. B. Alazmi and K. Vafai, Constant wall heat flux boundary condition in porous media under local thermal non-equilibrium conditions, Int. J. of Heat and Mass Transfer, vol.45, pp. 3071–3087, 2002.

41. P. X. Jiang, B. X. Wang and Z. P. Ren, Experimental research of fluid flow and convection heat transfer in plate channels filled with glass or metallic particles, Experimental Thermal and Fluid Sciences, vol. 20, pp. 45-54, 1999.

42. P. X. Jiang, B. X. Wang, D. A. Luo, and Z. P. Ren, Fluid flow and convection and heat transfer in a vertical porous annulus. Numerical Heat Transfer A, vol. 30, pp. 305–320, 1996.

43. P. X. Jiang, Z. P. Ren, and B. X. Wang, Numerical simulation of forced convection heat transfer in porous plate channels using thermal equilibrium and nonthermal equilibrium models, Numerical Heat Transfer Part A, vol. 35, pp. 99–113, 1999.

44. M. Lacroix, Contact melting of a phase change material inside a heated parallelepedic capsule, Energy conversion and management, vol. 42, pp. 35–47, 2001.

45. D. Groulx and W. Ogoh, Solid-liquid phase change simulation applied to a cylindrical latent heat energy storage system. In Excerpt from the proceeding of the COMSOL conference, Boston, USA, 2009.

46. W. Foudhil, B. Dhifaoui, S. Ben Jabrallah, A. Belghith, J. P. Corriou, Numerical and experimental study of convective heat transfer in a vertical porous channel using a non-equilibrium model. Journal of Porous Media, vol. 15(6), pp. 531-547, 2012.

47. S. Citherlet and J. Bony, Combi-Système avec Matériaux à Changement de Phase. Rapport final 2006, l'Office fédéral de l'énergie OFEN, Institution mandaté, École d'Ingénierie et de Gestion du Canton de Vaud (HEIG-VD/LESBAT), 2006.

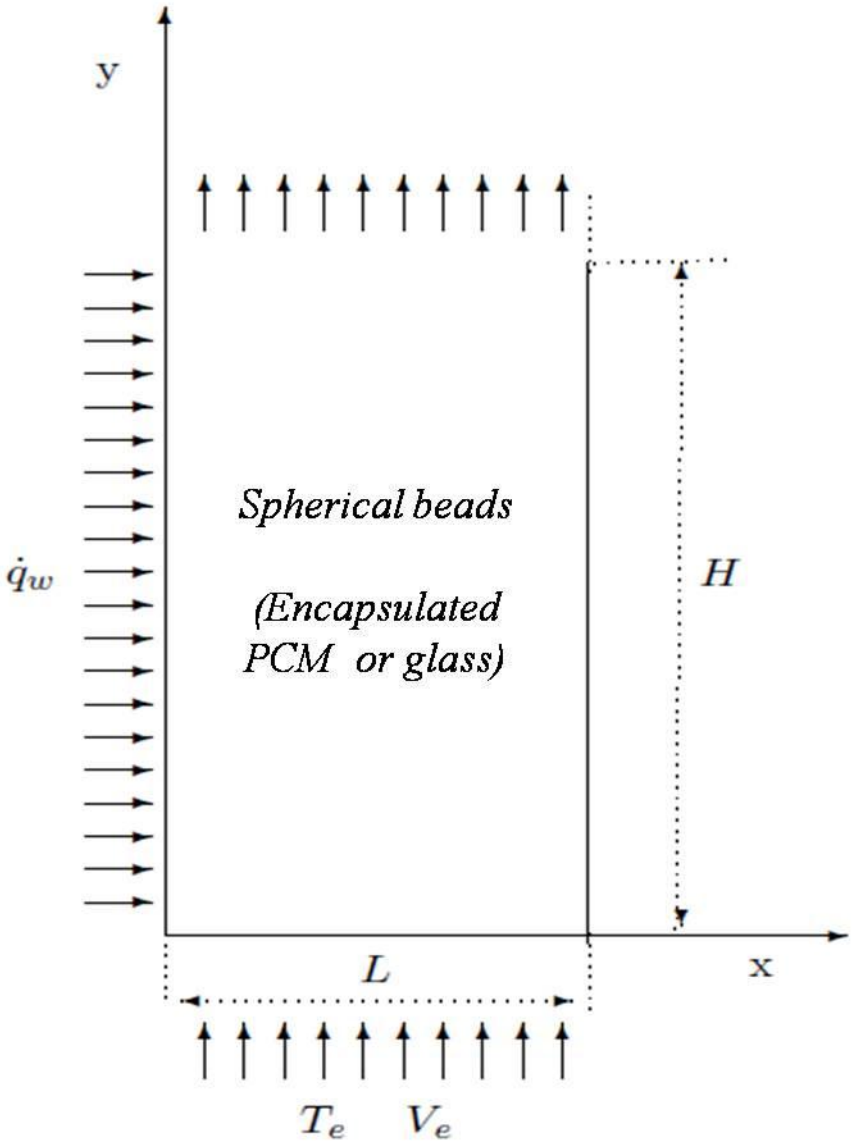

Fig. 1: Schematic representation of the two-dimensional porous channel

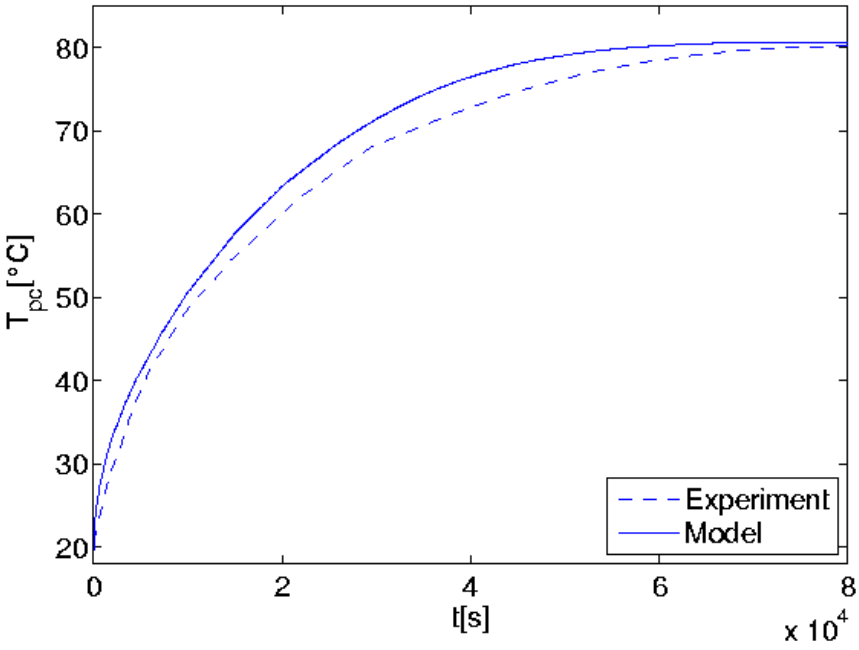

Fig. 2: Comparison of the numerical predictions with experimental results (Dhifaoui [8]) for a vertical channel filled with glass beads: variation of temperature at the heated wall with time ($\dot{q}_w = 250\ \mathrm{Wm}^{-2}$, $d = 10^{-2} m$, $L = 0.07$ m, $H = 0.4$ m $T_e = 293$ K)

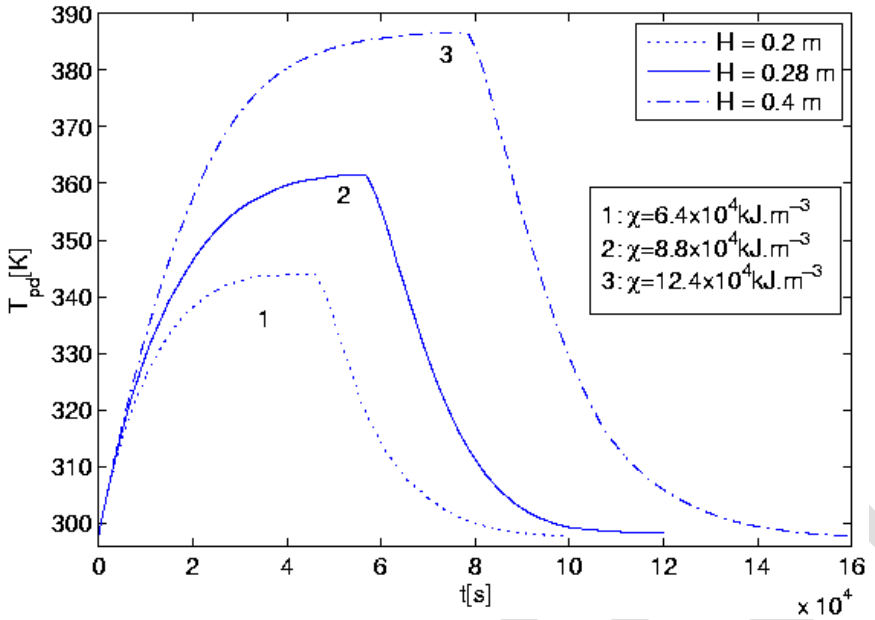

(a)

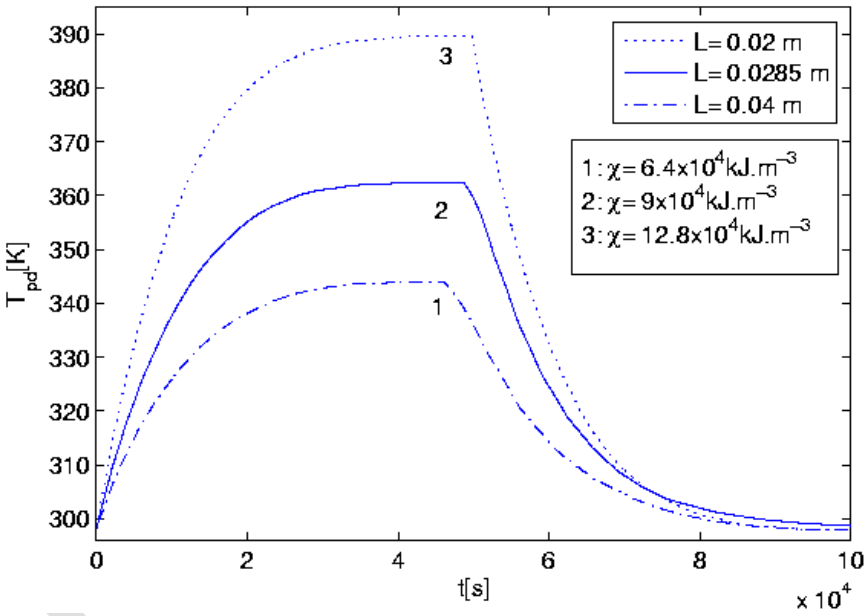

(b)

Fig. 3: Average temperature of the porous medium:

a) for different heights, H; b) for various widths, L

($\dot{q}_w = 250\ \mathrm{Wm}^{-2}$, $d = 10^{-2} m$, $m_f = 1.2\times10^{-4}\ \mathrm{kg\cdot s^{-1}}$, $T_e = 298\ \mathrm{K}$)

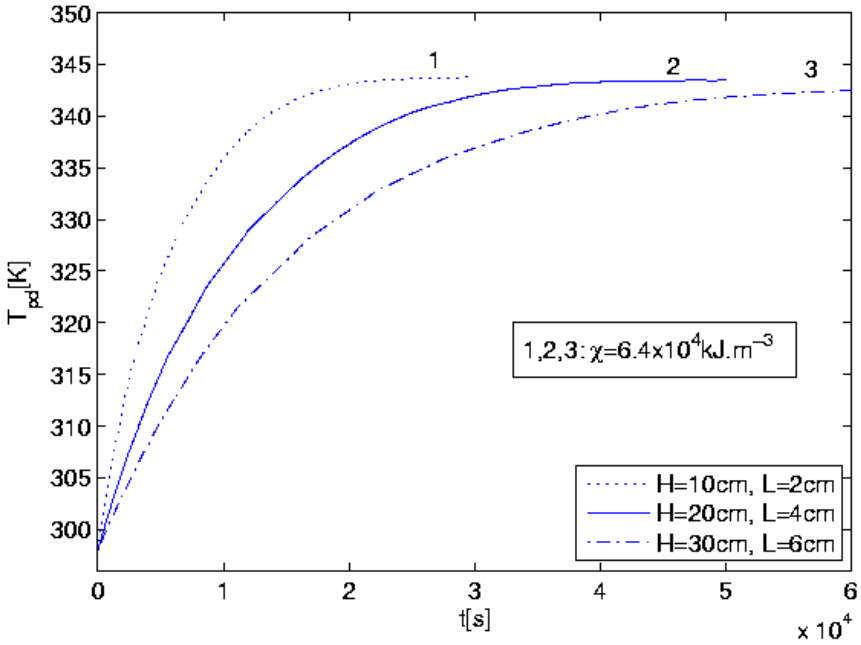

Fig. 4: Average temperature evolution for charging process for various height and width with a constant aspect ratio, A

($\dot{q}_w = 250\ \mathrm{Wm^{-2}}$, $A = 5$, $m_f = 1.2\times10^{-4}\ \mathrm{kg\cdot s^{-1}}$, $d = 10^{-2} m$, $T_e = 298\ \mathrm{K}$)

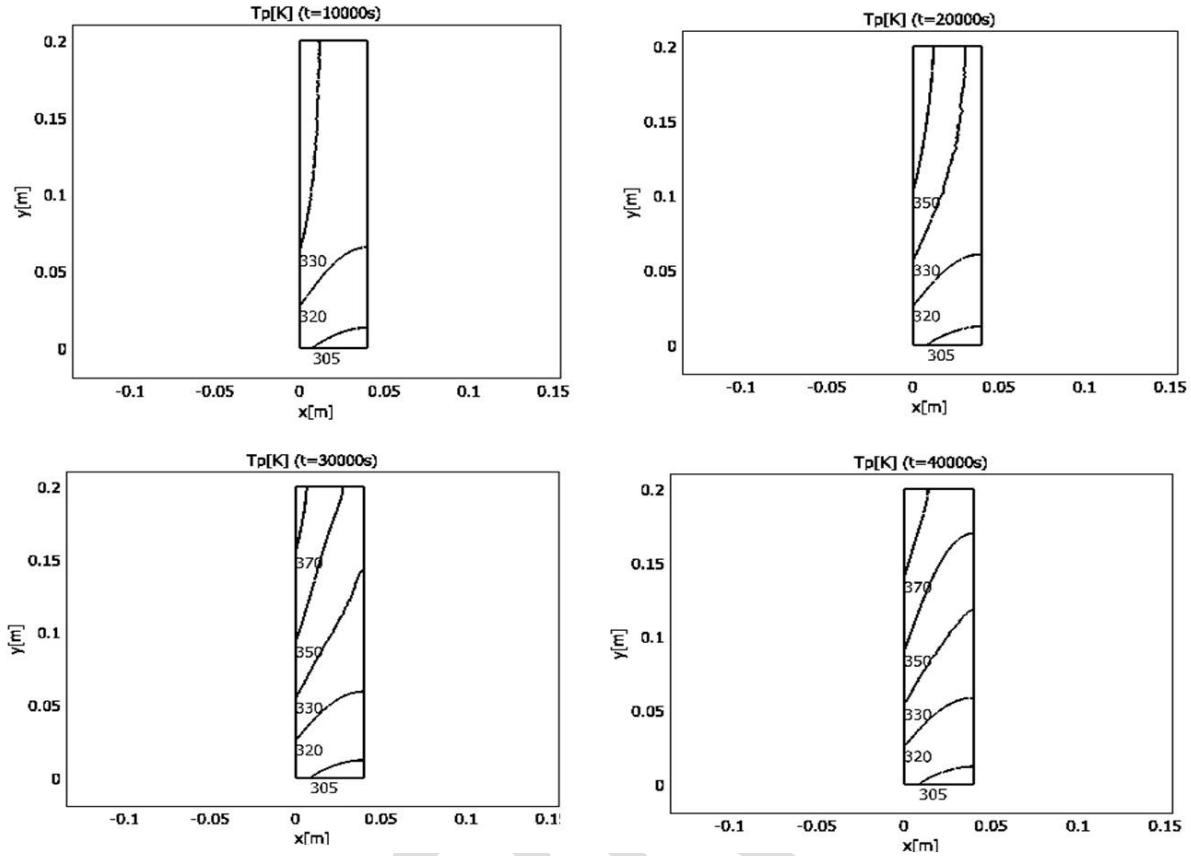

Fig. 5: Temperature variation of the PCM in the porous medium through the charging phase ($\dot{q}_w = 250\ \mathrm{Wm^{-2}}$, $A = 5$, $d = 10^{-2} m$, $m_f = 1.2\times10^{-4}\ \mathrm{kg.s^{-1}}$, $T_e = 298\ \mathrm{K}$)

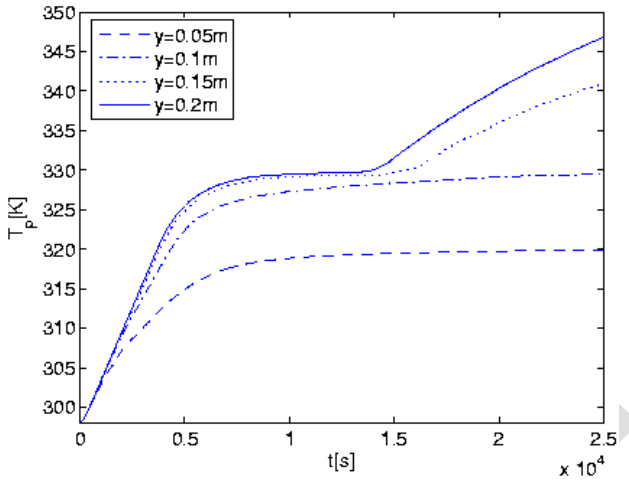

(a)

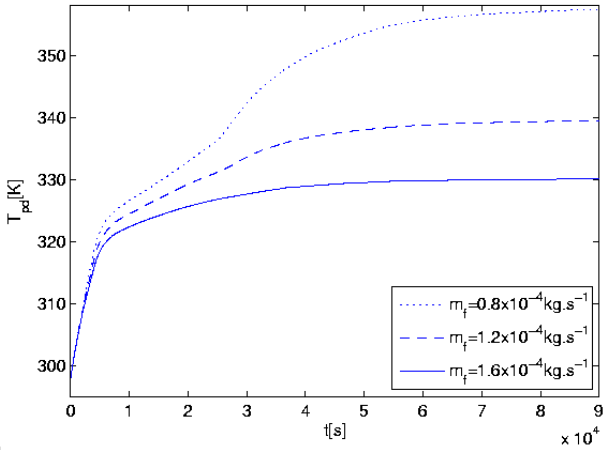

(b)

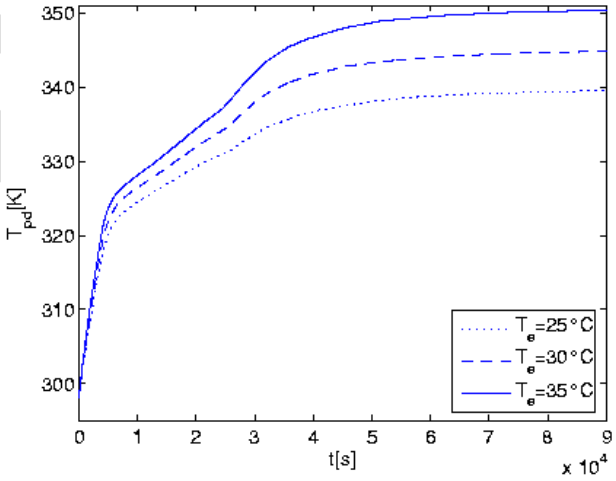

(c)

Fig. 6: Evolution of temperature in the channel over time for different: a) heights in the cavity, *y*; b) mass flow rates m_f, c) inlet temperature, T_e

($\dot{q}_w = 250\ \mathrm{Wm}^{-2}$, $A = 5$, $d = 10^{-2} m$, , $T_e = 298\ \mathrm{K}$)

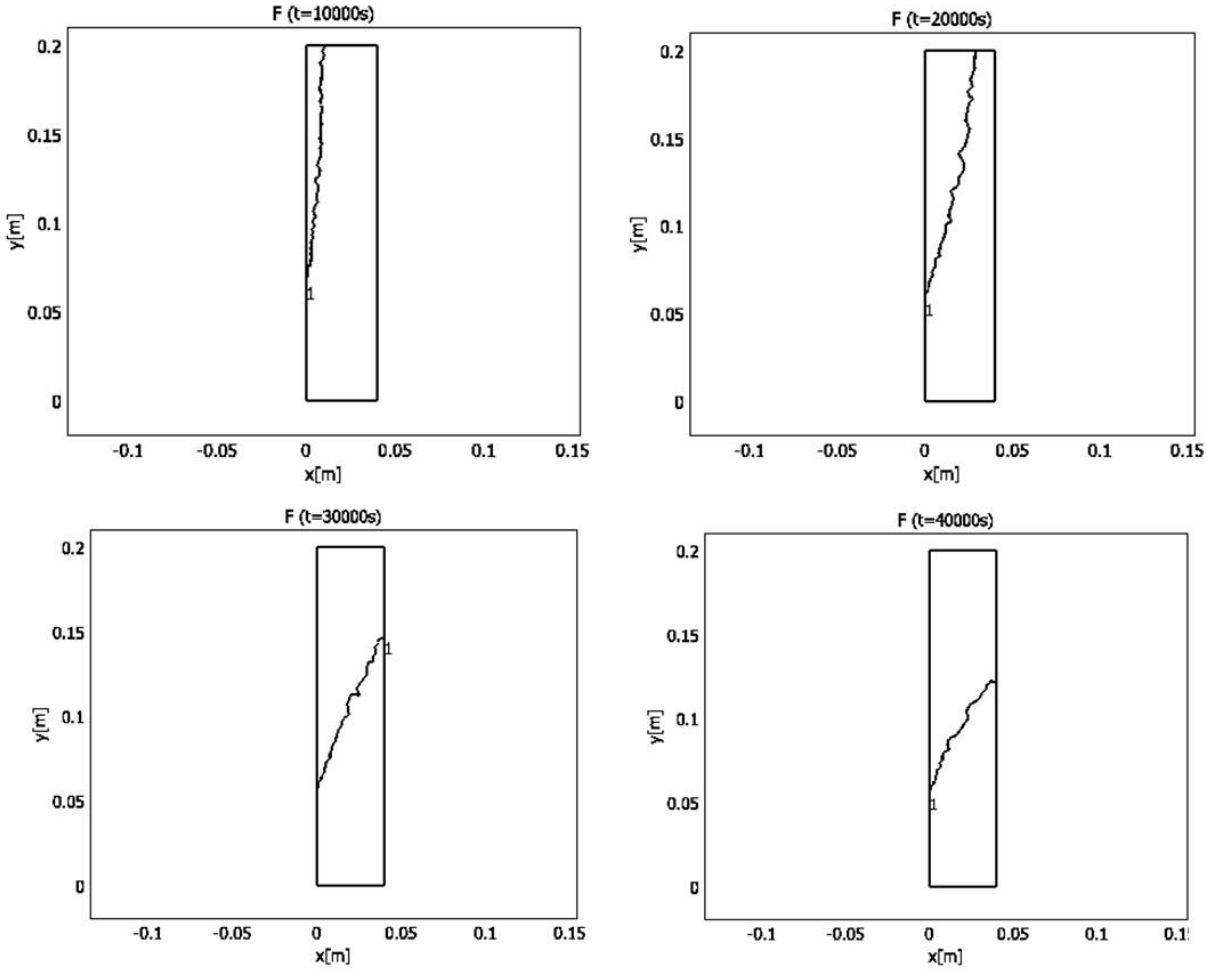

Fig. 7: Evolution of the fusion front in the porous domain trough the charging phase ($\dot{q}_w = 250\ \mathrm{Wm^{-2}}$, $A = 5$, $d = 10^{-2} m$, $m_f = 1.2\times10^{-4}\ \mathrm{kg.s^{-1}}$, $T_e = 298\ \mathrm{K}$)

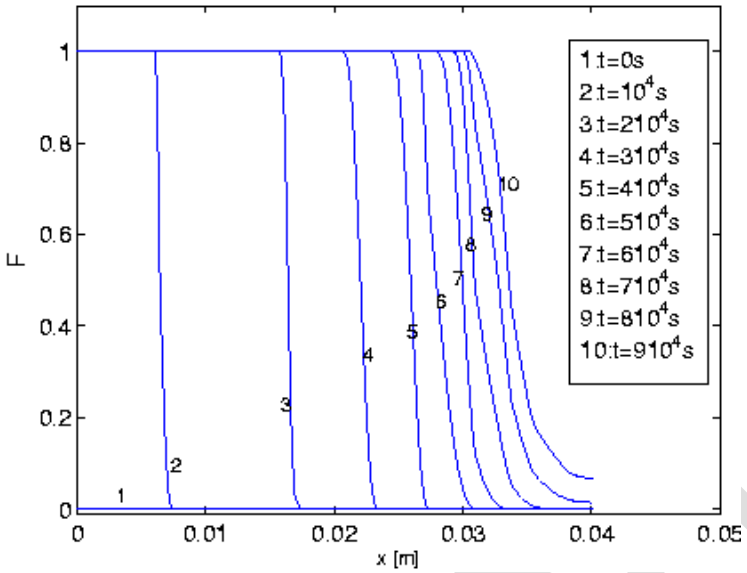

Fig. 8: Evolution with time of the melting front F at mid-height

($\dot{q}_w = 250\ \mathrm{Wm^{-2}}$, $A = 5$, $d = 10^{-2} m$, $m_f = 1.2\times10^{-4}\ \mathrm{kg.s^{-1}}$, $T_e = 298\ \mathrm{K}$)

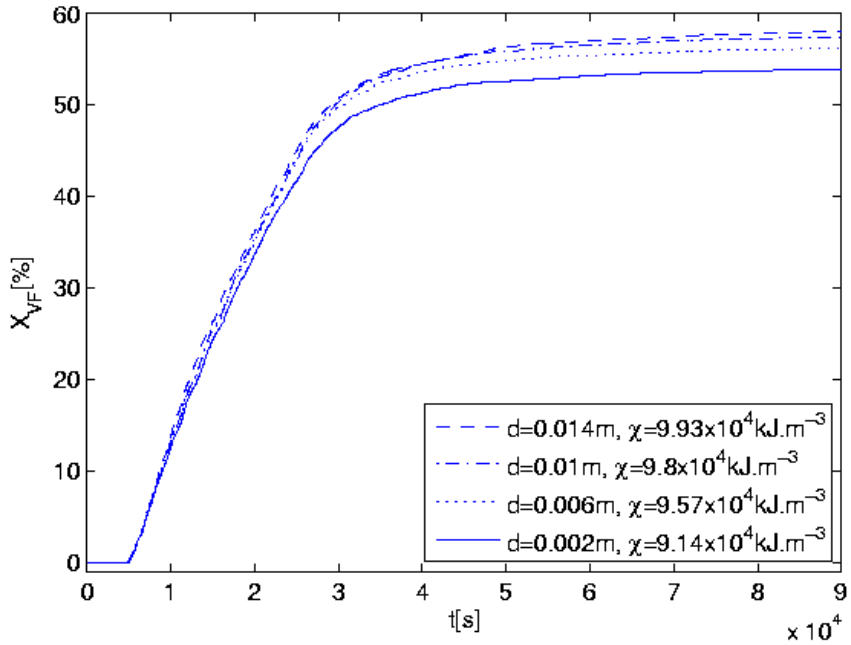

(a)

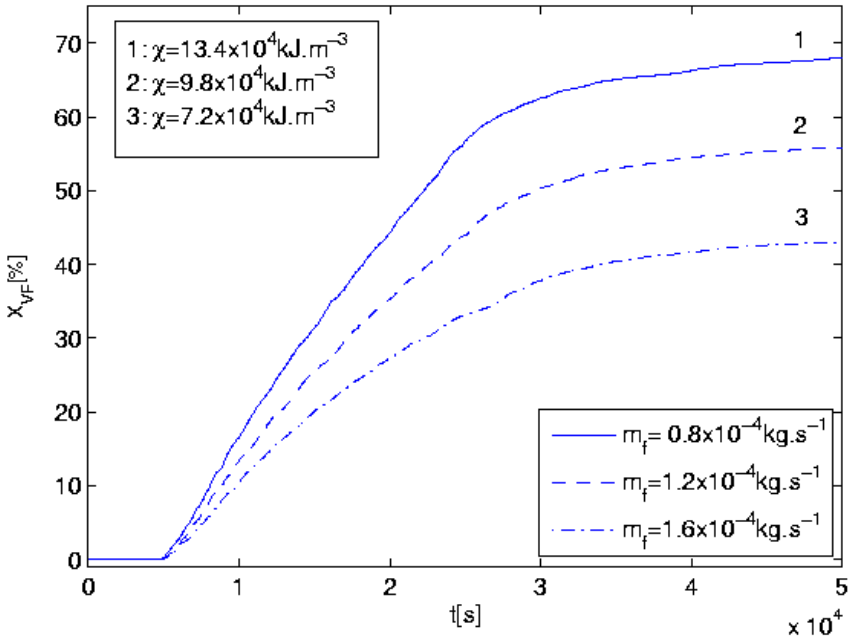

(b)

Fig. 9: Variation of the melted volume fraction, X, with respect to time for different: (a) capsule diameter, d; (b) mass flow rates, m_f.

($\dot{q}_w = 250\ \mathrm{Wm^{-2}}$, $A = 5$, $T_e = 298\ \mathrm{K}$)

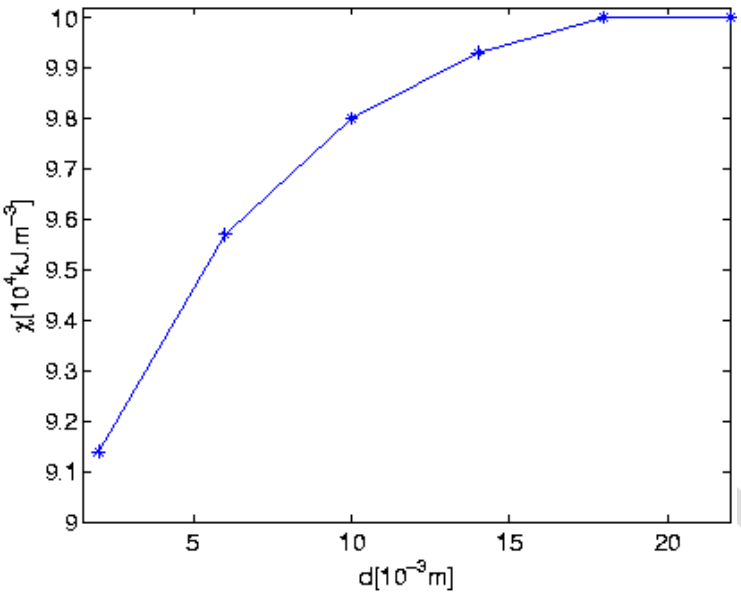

Fig. 10: Variation of the stored energy with the capsule diameter

($\dot{q}_w = 250\ \mathrm{Wm^{-2}}$, $A = 5$, $m_f = 1.2\times10^{-4}\ \mathrm{kg.s^{-1}}$, $T_e = 298\ \mathrm{K}$)

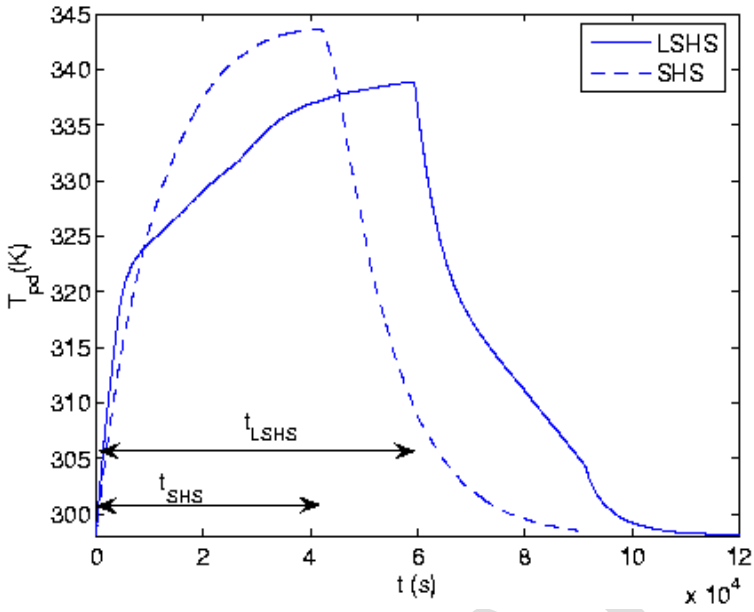

Fig. 11: Comparison between sensible heat (SHS) and latent heat (LSHS) storage system: Average temperature of the porous medium.

t_{SHS}:storage time for sensible heat system, t_{LSHS}:storage time for latent heat system

($\dot{q}_w = 250\ \mathrm{Wm^{-2}}, d = 0.01\ \mathrm{m},\ A = 5,\ m_f = 1.2\times10^{-4}\ \mathrm{kg.s^{-1}},\ T_e = 298\ \mathrm{K}$)

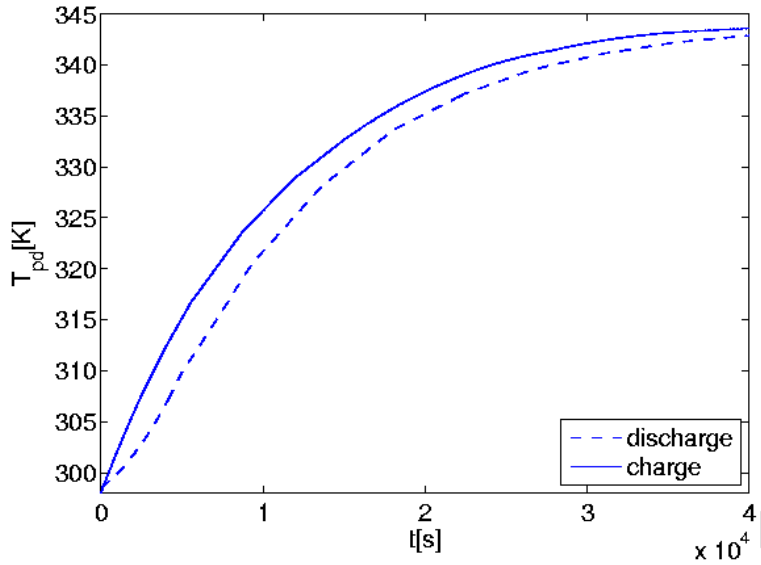

(a)

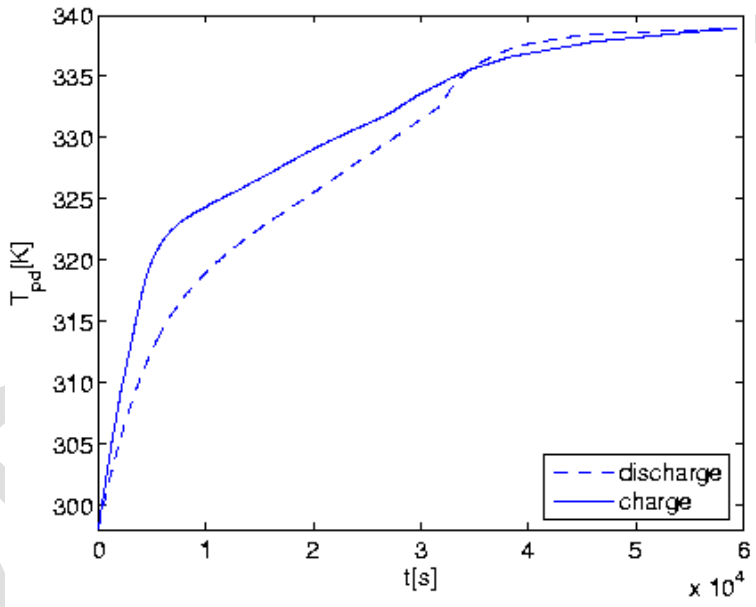

(b)

Fig. 12: Average temperature evolution of the porous medium for charge and discharge: a) glass bead; (b) phase change material.

($\dot{q}_w = 250\ \mathrm{Wm^{-2}}, d = 0.01\ \mathrm{m}, A = 5, m_f = 1.2\times10^{-4}\ \mathrm{kg.s^{-1}}, T_e = 298\ \mathrm{K}$)

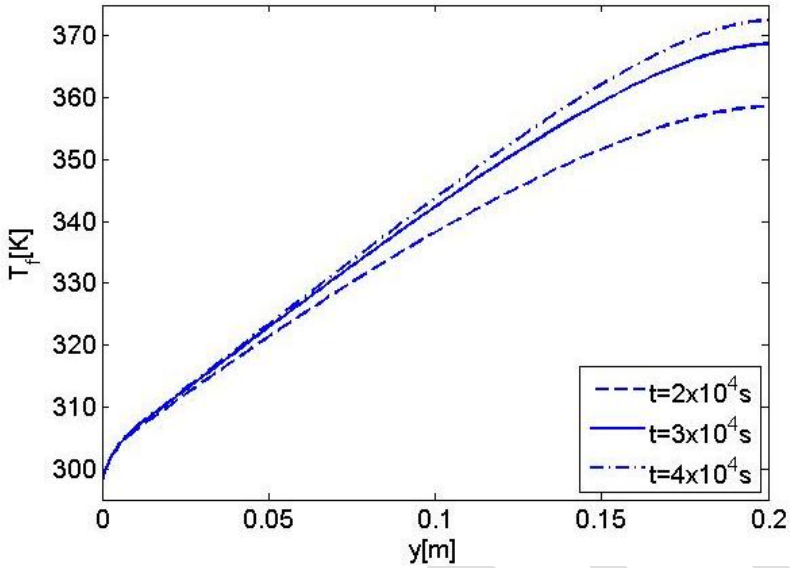

(a)

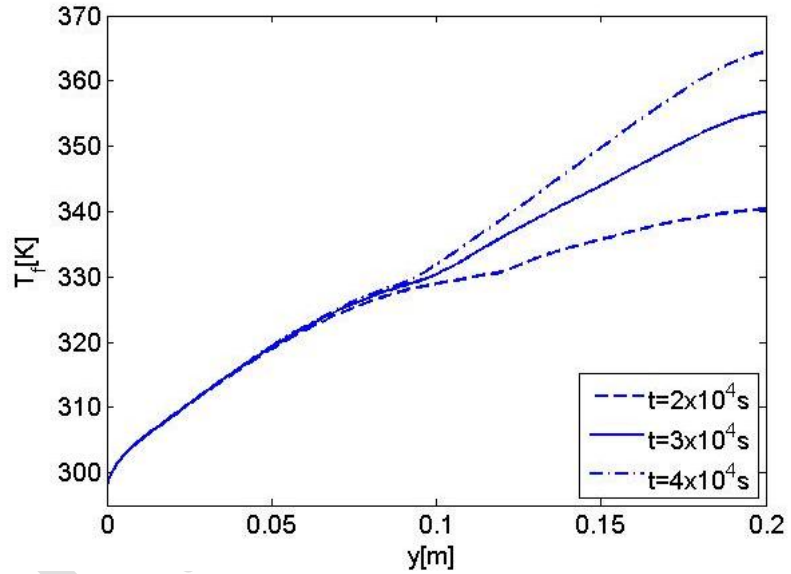

(b)

Fig. 13: Evolution of the fluid (air) temperature as a function of height, *y*, at the center (*x=L/2*) of the channel filled with glass beads for several periods of time.

($\dot{q}_w = 250\ \mathrm{Wm^{-2}}, d = 0.01\ \mathrm{m}, A = 5, m_f = 1.2\times10^{-4}\ \mathrm{kg.s^{-1}}, T_e = 298\ \mathrm{K}$)

Table 1: Physical properties of the porous medium

	λ [$W \cdot m^{-1} \cdot K^{-1}$]	ρ [$kg \cdot m^{-3}$]	Cp [$J \cdot kg^{-1} \cdot K^{-1}$]	ν [$m^2 \cdot s^{-1}$]
Air	0.026	1.127	1007	2.4×10^{-5}
Glass	0.7	2700	840	—

Table 2: Physical characteristics of paraffin in solid and liquid phase

Physical characteristics	Solid phase	Liquid phase
Temperature of fusion, T_{fus} (K)	330	
Latent heat of fusion, L_{fus} (kJ.kg^{-1})	213	
Density, ρ (kg.m^{-3})	861	778
Specific heat, Cp (J.kg^{-1}.K^{-1})	1851	2384
Thermal conductivity, λ (W.m^{-1}.K^{-1})	0.4	0.15
Ratio of the conductivity capsules-air (λ_p/λ_f)	15.38	5.77

Table 3: Comparison between the two storage modes for various inlet temperature differences

($\dot{q}_w = 250\ \mathrm{Wm^{-2}}$, $m_f = 1.2\times10^{-4}\ \mathrm{kg.s^{-1}}$, $A = 5$, $d = 10^{-2} m$, $t_{stock} = 4\times10^{4}\ \mathrm{s}$)

	$\Delta T = 0^{\circ}C$	$\Delta T = 5^{\circ}C$	$\Delta T = 10^{\circ}C$	$\Delta T = 15^{\circ}C$
$\chi_{(SHS)}(10^4 kJ.m^{-3})$	6.4	7.23	8.05	8.89
$\chi_{(LSHS)}(10^4 kJ.m^{-3})$	9.8 ($X_{VF} = 55.62\%$)	11.11 ($X_{VF} = 62.6\%$)	12.4 ($X_{VF} = 69.41\%$)	13.8 ($X_{VF} = 75.76\%$)
$\frac{\chi_{(LSHS)} - \chi_{(SHS)}}{\chi_{(SHS)}}$ (%)	53.1	53.7	54.0	55.0

Table 4: Comparison between the two storage modes for various particles diameters

($\dot{q}_w = 250\ \mathrm{Wm^{-2}}, m_f = 1.2\times10^{-4}\ \mathrm{kg.s^{-1}},\ A = 5,\ \Delta T = 0^{\circ}C,\ t_{stock} = 5.10^4 s$)

	$d = 2.10^{-3} m$	$d = 6.10^{-3} m$	$d = 10^{-2} m$	$d = 1.4\times10^{-2}\ \mathrm{m}$
$\chi_{(SHS)}(10^4 kJ.m^{-3})$	5.97	6.29	6.4	6.46
$\chi_{(LSHS)}(10^4 kJ.m^{-3})$	9.14 ($X_{VF} = 52.6\%$)	9.57 ($X_{VF} = 54.83\%$)	9.8 ($X_{VF} = 55.62\%$)	9.93 ($X_{VF} = 56.29\%$)
$\frac{\chi_{(LSHS)} - \chi_{(SHS)}}{\chi_{(SHS)}}$ (%)	53	52.14	53.12	53.71

Table 5: Comparison between the two storage modes for various mass flow rates

($\dot{q}_{fw} = 250\ \mathrm{Wm}^{-2}, d = 10^{-2} m, A = 5,\ \Delta T = 0^{\circ} C, t_{stock} = 5.10^{4} s$)

	$m_f = 0.810^{-4} kg.s^{-1}$	$m_f = 1.210^{-4} kg.s^{-1}$	$m_f = 1.610^{-4} kg.s^{-1}$
$\chi_{(SHS)}(10^4 kJ.m^{-3})$	9.3	6.4	4.81
$\chi_{(LSHS)}(10^4 kJ.m^{-3})$	13.4 ($X_{VF} = 68\%$)	9.8 ($X_{VF} = 55.62\%$)	7.2 ($X_{VF} = 43\%$)
$\frac{\chi_{(LSHS)} - \chi_{(SHS)}}{\chi_{(SHS)}}$ (%)	44	53.1	49.6